Available online at www.sciencedirect.com

SciVerse ScienceDirect

Ceramics International 38 (2012) 6843–6847

CERAMICS INTERNATIONAL

www.elsevier.com/locate/ceramint

Fabrication and characterization of a dual layer ceramic interconnect on a porous NiO-YSZ anode support

Mi Young Yoon[a], Byung-Hyun Choi[b], Rak Hyun Song[c], Hae Jin Hwang[a,*]

[a]School of Materials Science and Engineering, Inha University, 253 Yonghyun-dong, Nam-gu, Incheon 402-751, Republic of Korea
[b]Korea Institute of Ceramic Engineering and Technology, 233-5 Gasan-dong, Guemcheon-gu, Seoul 153-801, Republic of Korea
[c]Korea Institute of Energy Research, 152 Gajeong-ro, Yuseong-gu, Daejeon 305-343, Republic of Korea

Received 8 March 2012; received in revised form 15 May 2012; accepted 25 May 2012
Available online 30 May 2012

Abstract

An $La_{0.8}Sr_{0.2}MnO_3$ (LSM)/$Sr_{0.88}Y_{0.08}TiO_3$ (SYT) dual layer interconnect was coated on an NiO-YSZ porous support via screen printing and co-firing processes. SYT and LSM single phase powders were synthesized by solid state reaction and Pechini method, respectively. The thickness of the dual layer was approximately 200 μm. The LSM/SYT dual layer showed a good gas-tightness and had a uniform microstructure without cracks, delamination or warpage. No atomic inter-diffusion between the dual layer and the NiO-YSZ support was detected, suggesting that SYT is phase compatible with NiO-YSZ. The area specific resistance (ASR) of the LSM/SYT/Ni-YSZ sample was 0.19 Ω cm^2 at 800 °C under oxidizing/reducing atmospheres; this value was lower than that of the SYT/Ni-YSZ sample.

Keywords: D. Perovskite; Solid oxide fuel cells; Interconnect; Area specific resistance

1. Introduction

Interconnects for solid oxide fuel cells (SOFCs) are used to physically separate and electrically connect the anode and cathode of adjacent cells. Interconnect materials must satisfy the following requirements: 1) interconnects should quickly and easily transfer electrons generated from the anode side to adjacent cathode side, 2) interconnects should be stable in chemical composition and phase under oxidizing and reducing atmospheres, 3) interconnects should have a dense microstructure to prevent the direct combination of oxygen and hydrogen [1]. Among the ceramic interconnect materials that can satisfy these requirements, strontium or calcium-doped $LaCrO_3$-based materials have been extensively studied [2,3]. Although they have a high electrical conductivity, adequate thermal expansion coefficient (TEC) and phase stability, strontium-doped $LaCrO_3$ suffers from poor sinterability and nonlinear thermal expansion behavior. On the other hand, calcium migration is a serious problem when calcium-doped $LaCrO_3$ is coated on the NiO-YSZ of an anode-supported flat tubular SOFC [4]. In addition, chromium-containing interconnects can cause the formation of volatile Cr (VI) species such as CrO_3 and $CrO_2(OH)_2$ under SOFC operating conditions, which may diffuse to the cathode and then increase the polarization resistance. Therefore, chromium-free interconnect materials have been proposed as alternatives to $LaCrO_3$-based perovskite materials [5,6]. Recently, much attention has been paid to rare-earth-doped $SrTiO_3$-based perovskites due to their high electrical conductivity and phase stability under a reducing atmosphere [7,8].

In this study, we tried to develop the interconnect material which can be applied to flat tubular SOFCs. Y-doped $SrTiO_3$ was chosen as an interconnect material because Y-doped $SrTiO_3$ has the highest electrical conductivity among rare-earth-doped $SrTiO_3$ [9]. However, the electrical conductivity of Y-doped $SrTiO_3$ in air is about two orders of magnitude lower than it is in H_2. Since

*Corresponding author. Tel.: +82 32 860 7521; fax: +82 32 862 4482.
E-mail address: hjhwang@inha.ac.kr (H.J. Hwang).

0272-8842/$36.00
http://dx.doi.org/10.1016/j.ceramint.2012.05.084

one side of the interconnect (Y-doped $SrTiO_3$) is exposed to air, a blocking layer that can reduce the oxygen potential is needed. In this regard, a dual-layered interconnect consisting of Y-doped $SrTiO_3$ for the H_2 side and Sr-doped $LaMnO_3$ for the air side might be a promising candidate. Y-doped $SrTiO_3$ and Sr-doped $LaMnO_3$ layers were coated on a porous NiO-YSZ support by screen printing and subsequent co-firing. Phase stability, microstructure and electrical properties were examined.

2. Experimental procedure

An $Sr_{0.88}Y_{0.08}TiO_3$ (SYT) powder was synthesized by solid state reaction. Strontium carbonate ($\geq 99.9\%$, Aldrich), yttrium oxide (99.99%, Aldrich) and titanium oxide (99.9%, High Purity Chemicals) were used as starting materials. Strontium carbonate was heated in air at 200 °C to eliminate the hydration effect. The starting materials were mixed for 24 h by ball-milling in a plastic jar containing ethyl alcohol. After drying, the powder was calcined at 1000 °C in air and then reduced at 1400 °C for 3 h under 5% H_2/Ar atmosphere.

An $La_{0.8}Sr_{0.2}MnO_3$ (LSM) powder was synthesized by the Pechini method. Lanthanum (III) acetate hydrate (99.9%, Aldrich), strontium acetate (99.9%, Aldrich), manganese (II) acetate tetrahydrate (99%, Aldrich), citric acid (99.5%, Junsei) and ethylene glycol (99.5%, Kanto Chemical Co., Inc.) were used as starting materials. The molar ratio of total metal ions, citric acid and ethylene glycol was 1:2:2. After metal acetates were dissolved in distilled water, an aqueous citric acid and ethylene glycol solution were sequentially added to the solution containing metal ions, which was stirred at 50 °C for 1 h to obtain a clear solution. Then, the solution was heated up to 80 °C and kept for 12 h to remove the water that was produced by the polyesterification between ethylene glycol and citric acid. The solution was transformed into a thick deep-brown gel, which was dried overnight in an oven that had been pre-heated to 250 °C; solution subsequently formed a sponge-like polymeric resin. Finally, this resin was calcined at 700 °C in air for 5 h.

The LSM/SYT dual layer was fabricated by screen printing and co-firing. Each paste was made by mixing the obtained powders into the vehicle. The SYT layer was coated on a porous NiO-YSZ anode support and then the LSM layer was coated on the SYT/NiO-YSZ. The LSM/SYT/NiO-YSZ sample was co-fired at 1400 °C for 2 h in air. For comparison, the SYT/NiO-YSZ sample was also prepared by the same method described before.

Phase identification was carried out using an X-ray diffractometer (XRD, DMAX 2200, Rigaku, Japan) using CuKα radiation. For compositional analysis, the microstructure of the LSM/SYT dual layer was observed with a scanning electron microscope (SEM, JSM-5500, JEOL, Japan) equipped with an energy dispersive spectrometer (EDS). The gas tightness of the dual layer was confirmed by micro-gas chromatography (micro-GC) and with an oxygen sensor. The LSM and NiO-YSZ sides were exposed to air and N_2, respectively, and the oxygen concentration of the effluent gas from the NiO-YSZ support side was measured. The area specific resistance (ASR) of the dual layer was measured at 500–800 °C using a DC four-probe method. First, the LSM/SYT sample on the NiO-YSZ support was reduced at 850 °C for 3 h under 100% H_2 atmosphere. Then, H_2 and air were supplied to the Ni-YSZ and LSM/SYT sides, respectively.

3. Results and discussion

Although not shown in this paper, the XRD pattern of the LSM powder synthesized by the Pechini method showed that a single phase perovskite can be obtained after calcining the precursor ash at 700 °C for 5 h in air. Fig. 1 shows the XRD patterns of the powder samples that were synthesized from $SrCO_3$, Y_2O_3, and TiO_2 by solid state reaction. The XRD analysis revealed that the 1000 °C-calcined powder consisted of perovskite, pyrochlore ($Y_2Ti_2O_7$), and unreacted Y_2O_3 and TiO_2. When the powder sample was further heat-treated at 1400 °C in air, both Y_2O_3 and TiO_2 phases disappeared and the intensity of the peak corresponding to the pyrochlore phase increased. This result suggests that the unreacted Y_2O_3 and TiO_2 were consumed to produce the $Y_2Ti_2O_7$ phase. A rare earth-titanate pyrochlore formation often occurs when a powder mixture containing rare-earth and titanium oxides is calcined above 900 °C in air [10,11].

On the other hand, it was possible to obtain a single phase perovskite when the 1000 °C-calcined powder was given heat treatment at 1400 °C in 5% H_2/Ar, as can be seen in Fig. 1(c). The oxidation state of the Ti ion in the $Y_2Ti_2O_7$ pyrochlore phase is tetravalent. If $Y_2Ti_2O_7$ is reduced at low oxygen partial pressure, Ti^{4+} ions will be reduced to Ti^{3+}; also, for charge compensation, some oxygen is removed

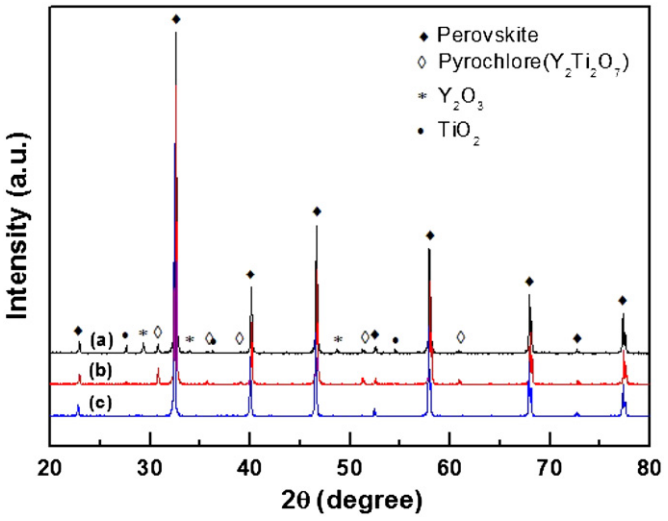

Fig. 1. XRD patterns of the SYT powder calcined at 1000 °C in air (a), subsequently heat-treated at 1400 °C in air (b) and heat-treated in 5% H_2/Ar (c).

from the crystal structure, leaving oxygen vacancies in the structure. Owing to such phenomena, yttrium titanate cannot maintain the pyrochlore structure and Y and Ti are dissolved into the $SrTiO_3$ perovskite. In addition, it was found that the color of the powder calcined in air was white, while that of the reduced powder was bluish–gray. As the reduction proceeded, the color became deeper, indicating that more Ti^{4+} ions had been reduced to Ti^{3+} ions [12].

Fig. 2 shows cross-section and surface images of the SYT and LSM/SYT layers coated on a porous NiO-YSZ support by screen printing and co-firing at 1400 °C for 2 h in air. Both the SYT and LSM layers have quite dense and uniform microstructures with thickness of about 100 μm. In addition, it appears that the SYT and LSM layers adhered well to the porous NiO-YSZ support and to the SYT, respectively, not showing cracks or delamination. As is evident in Fig. 2(c), the thickness of the LSM/SYT dual layer was about 200 μm. It is widely known that co-firing is a very cost-effective and simple method to make a supported SOFC [13]. However, many defects such as cracks, delamination and/or warpage may occur due to shrinkage or thermal expansion mismatch between cell components. The thermal expansion coefficients of SYT, LSM, and NiO-YSZ are 12.0, 11.8 and $11.5 \times 10^{-6}\,°C^{-1}$, respectively [14–16].

Fig. 3 shows EDS line analysis results for the LSM/SYT dual layer coated on the porous NiO-YSZ support. Strontium and titanium were not detected in the NiO-YSZ support, indicating the phase compatibility between the SYT and NiO-YSZ. In addition, there is no sign indicating the diffusion of the lanthanum and manganese in LSM into the SYT layer. Thus, it is thought that the SYT and LSM layers are phase compatible with the NiO-YSZ and SYT layers, respectively.

A leakage test was performed to confirm the gas tightness of the LSM/SYT dual layer. What we should not overlook is that perovskite materials tend to have an ionic conductivity due to oxygen vacancies, which conductivity can be created under a low oxygen partial pressure or for charge compensation. The ionic conductivity is very useful in case the perovskite is used as an SOFC cathode. However, in the case of interconnects, oxygen

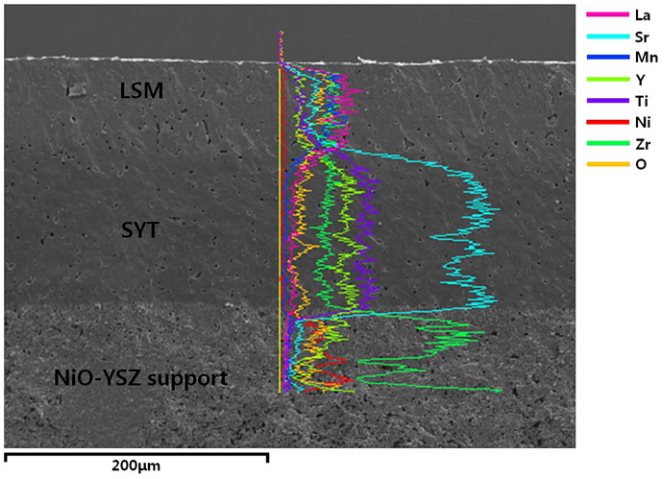

Fig. 3. EDS line profile of the LSM/SYT/NiO-YSZ sample.

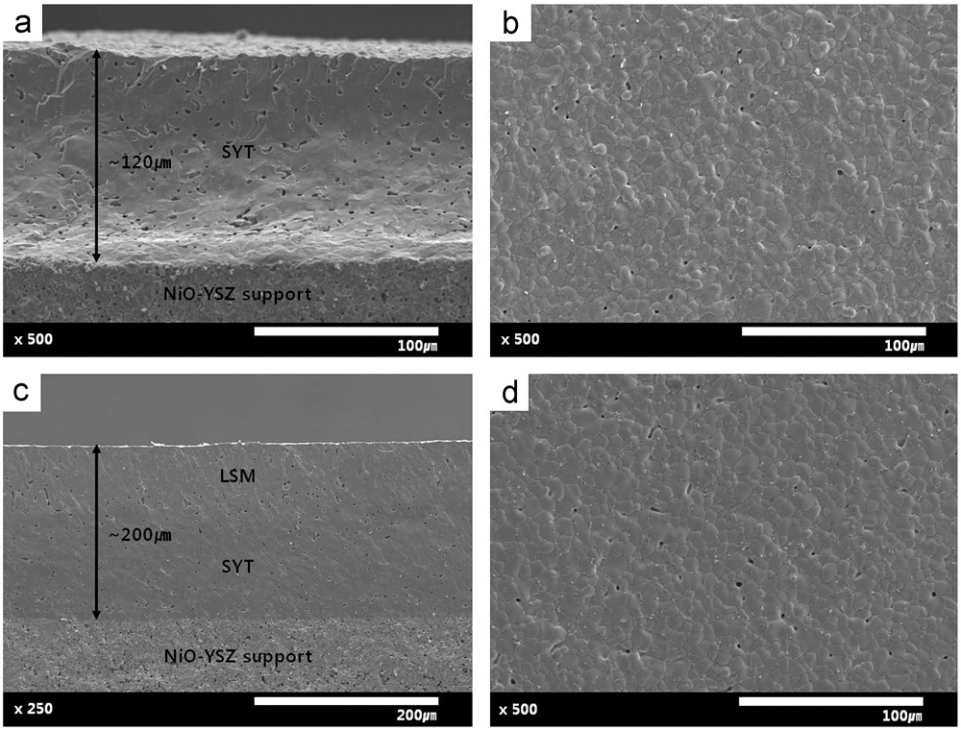

Fig. 2. SEM images of the SYT ((a) and (b)) and LSM/SYT layer ((c) and (d)) on an NiO-YSZ support: (a) and (c) are cross-sections, (b) and (d) are surfaces.

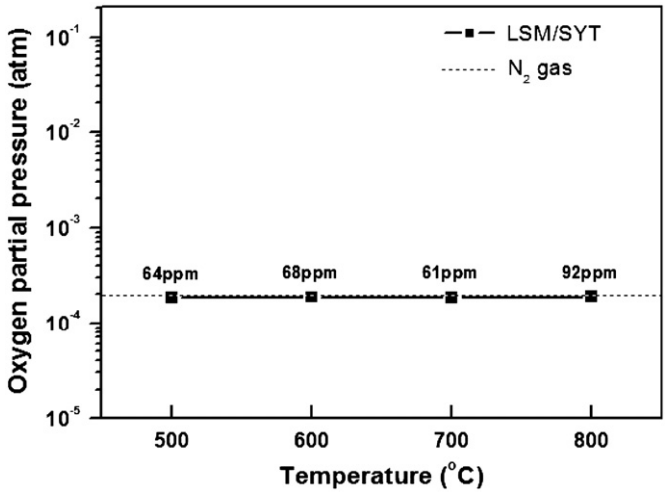

Fig. 4. Oxygen permeation of the LSM/SYT/NiO-YSZ sample.

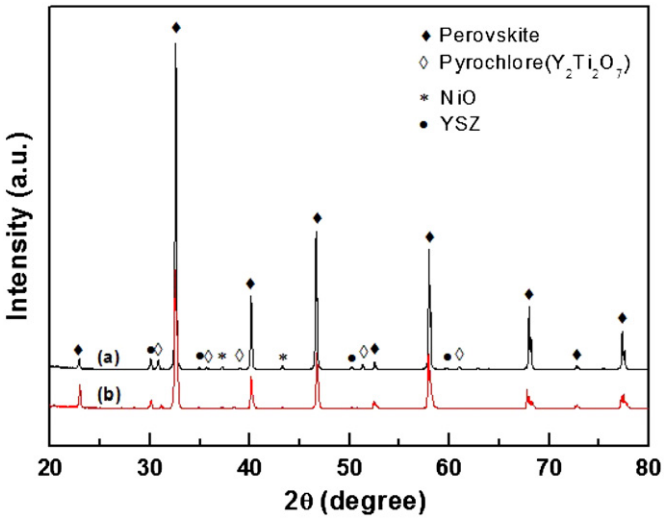

Fig. 5. XRD patterns of the SYT (a) and LSM/SYT (b) layers after co-firing in air.

supplied to the cathode can be transferred to the anode, this process causes a decrease in the open circuit voltage (OCV) and the cell performance. Therefore, it is important to examine the oxygen permeability of the LSM/SYT dual layer coated on the porous NiO-YSZ support. As can be seen in Fig. 4, the oxygen partial pressure of pure N_2 gas (dotted line) is approximately 10^{-4} atm. The oxygen partial pressure of the effluent gas from the Ni-YSZ support was almost the same as that of the N_2 gas in the temperature range 500–800 °C. These results indicate that the LSM/SYT dual layer coated on the NiO-YSZ porous support includes no pin-holes and has little oxygen ion diffusivity. Since $LaMnO_3$-based oxides have the extraordinary feature of oxygen excess under a high oxygen partial pressure, the oxygen vacancy concentration of the LSM is believed to be extremely low, suggesting poor oxygen ionic conductivity [17–19].

Fig. 5 shows the XRD patterns of the SYT and LSM/SYT layers. The SYT and LSM/SYT layers consist of perovskite as a major phase and NiO and YSZ, which are responsible for the NiO-YSZ support. No phase associated with the reaction between the coating layers and the NiO-YSZ support was detected. This result suggests that the LSM/SYT dual layer and the NiO-YSZ have good chemical compatibility. On the other hand, peaks that are attributed to the $Y_2Ti_2O_7$ pyrochlore were observed in the SYT layer. The pyrochlore is the phase that is formed as an unwanted second phase in a rare earth-doped perovskite under high oxygen partial pressure conditions. On the other hand, the pyrochlore phase almost disappeared in the LSM/SYT dual layer. It is considered that the LSM layer can suppress the formation of the pyrochlore phase in the SYT layer.

Fig. 6 shows the ASR of the SYT/Ni-YSZ and LSM/SYT/Ni-YSZ samples as a function of temperature. ASR was decreased with increasing temperature, which means that the electrical behavior of the two samples was governed by the SYT or the LSM/SYT layer. In addition,

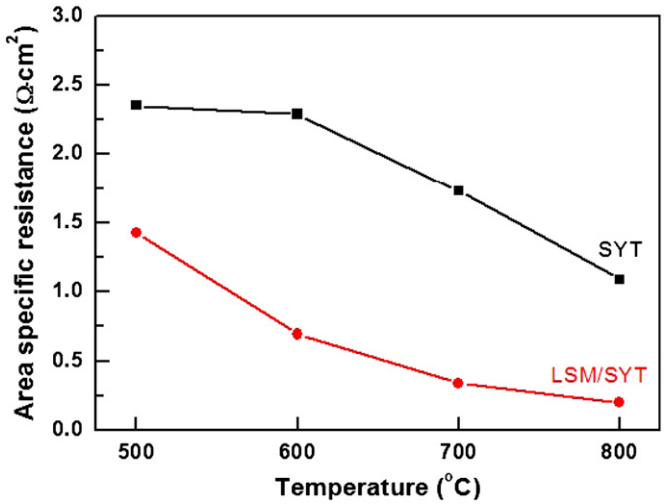

Fig. 6. ASR of the SYT/Ni-YSZ and LSM/SYT/Ni-YSZ samples as a function of temperature.

since the resistance of the Ni-YSZ support is much lower than those of the SYT or the LSM/SYT layers, the ASR of the sample may be caused by the SYT or the LSM/SYT layer. The ASR of the sample with the LSM/SYT dual layer was much lower than that of the sample with the SYT layer. The ASR of the LSM/SYT/Ni-YSZ sample was 0.19 Ω cm^2 at 800 °C. SYT is an n-type semiconductor and shows high electrical conductivity under a reducing atmosphere. The high ASR value observed in the SYT/Ni-YSZ sample may be responsible for the high oxygen partial pressure exposed to one side of the SYT layer. On the other hand, in the case of the LSM/SYT/Ni-YSZ sample, the SYT layer is covered by the LSM, which shows p-type semiconductivity. Thus the dual layer containing the LSM can result in a reduced electrical resistance under an oxidizing atmosphere. According to works in the literature, the ASR value of interconnects for SOFCs must be lower

than 0.1 $\Omega\,cm^2$ [20]. Although the ASR of the LSM/SYT/Ni-YSZ sample is slightly higher than this value, it can be improved further by reducing the thickness of the coating layers or modifying the interface between the layers.

4. Conclusions

An LSM/SYT dual layer on a porous NiO-YSZ support was fabricated via screen printing and co-firing. Both the SYT and LSM layers had dense and uniform microstructures without cracks, delamination or warpage. No sign of interdiffusion between the layers was detected after co-firing, suggesting good chemical compatibility between the LSM/SYT dual layer and the NiO-YSZ support. The LSM/SYT dual layer showed excellent resistance to oxygen permeation. The LSM/SYT dual layer was very effective at reducing the ASR of the sample since the LSM and SYT layers were exposed to air and H_2, respectively. On the other hand, the SYT/Ni-YSZ sample showed a higher ASR value than did the sample with the dual layer.

Acknowledgments

This research was supported by a grant from the Fundamental R&D Program for Core Technology of Materials funded by the Ministry of Knowledge Economy, Republic of Korea. Part of this work was supported by the National Research Foundation of Korea (NRF) grant funded by the Korea government (MEST) (no. 2011-0005103).

References

[1] W.Z. Zhu, S.C. Deevi, Development of interconnect materials for solid oxide fuel cells, Material Science and Engineering: A 348 (2003) 227–243.

[2] Y.-J. Yang, T.-L. Wen, H. Tu, D.-Q. Wang, J. Yang, Characteristics of lanthanum strontium chromite prepared by glycine nitrate process, Solid State Ionics 135 (2000) 475–479.

[3] S. Wang, B. Lin, K. Xie, Y. Dong, X. Liu, G. Meng, Low temperature sintering ability and electrical conductivity of SOFC interconnect material $La_{0.7}Ca_{0.3}Cr_{0.97}O_3$, Journal of Alloys and Compounds 468 (2009) 499–504.

[4] G.-Y. Lee, R.-H. Song, J.-H. Kim, D.-H. Peck, T.-H. Lim, Y.-G. Shul, D.-R. Shin, Properties of Cu, Ni, and V doped-$LaCrO_3$ interconnect materials prepared by Pechini, ultrasonic spray pyrolysis and glycine nitrate processes for SOFC, Journal of Electroceramics 17 (2006) 723–727.

[5] M.-J. Tsai, C.-L. Chu, S. Lee, $La_{0.6}Sr_{0.4}Co_{0.2}Fe_{0.8}O_3$ protective coatings for solid oxide fuel cell interconnect deposited by screen printing, Journal of Alloys and Compounds 489 (2010) 576–581.

[6] L.L. Zheng, J.J. Li, M.S. Li, Y.C. Zhou, Investigation on the properties of Nb and Al doped Ti_3SiC_2 as a new interconnect material for IT-SOFC, International Journal of Hydrogen Energy 37 (2012) 1084–1088.

[7] Y. Xu, S. Wang, R. Liu, T. Wen, Z. Wen, A novel bilayered $Sr_{0.6}La_{0.4}TiO_3/La_{0.8}Sr_{0.2}MnO_3$ interconnector for anode-supported tubular solid oxide fuel cell via slurry-brushing and co-sintering process, Journal of Power Sources 196 (2011) 1338–1341.

[8] Z. Wang, M. Mori, Sintering characteristics and electrical conductivity of $(Sr1\text{-}xLa_x)TiO_3$ synthesized by the citric acid method, Journal of Fuel Cell Science and Technology 8 (2011) 051018-1-5.

[9] S. Hui, A. Petric, Electrical properties of yttrium-doped strontium titanate under reducing conditions, Journal of the Electrochemical Society 149 (2002) J1–J10.

[10] S.L. Swartz, T.R. Shrout, Fabrication of perovskite lead magnesium niobate, Materials Research Bulletin 17 (1982) 1245–1250.

[11] G.R. Fox, S.B. Krupanidhi, Dependence of perovskite/pyrochlore phase formation on oxygen stoichiometry in PLT thin films, Journal of Materials Research 9 (1994) 699–711.

[12] A. Ookubo, E. Kanezaki, K. Ooi, ESR, XRD, and DRS studies of paramagnetic Ti^{3+} ions in a colloidal solid of titanium oxide prepared by the hydrolysis of $TiCl_3$, Langmuir 6 (1990) 206–209.

[13] M. Liu, D. Dong, F. Zhao, J. Gao, D. Ding, X. Liu, G. Meng, High-performance cathode-supported SOFCs prepared by a single-step co-firing process, Journal of Power Sources 182 (2008) 585–588.

[14] S. Hui, A. Petric, Evaluation of yttrium-doped $SrTiO_3$ as an anode for solid oxide fuel cells, Journal of the European Ceramic Society 22 (2002) 1673–1681.

[15] F. Tietz, I.A. Raj, M. Zahid, D. Stöver, Electrical conductivity and thermal expansion of $La_{0.8}Sr_{0.2}(Mn, Fe, Co)O_{3-y}$ perovskites, Solid State Ionics 177 (2006) 1753–1756.

[16] P. Timakul, S. Jinawath, P. Aungkavattana, Fabrication of electrolyte materials for solid oxide fuel cells by tape-casting, Ceramics International 34 (2008) 867–871.

[17] T. Ishihara, Perovskite Oxide for Solid Oxide Fuel Cells, Springer, New York, 2009.

[18] J.W. Fergus, R. Hui, X. Li, D.P. Wilkinson, J. Zhang, Solid Oxide Fuel Cells: Materials Properties and Performance, CRC Press, Florida, 2009.

[19] F.W. Poulsen, Defect chemistry modelling of oxygen-stoichiometry, vacancy concentrations, and conductivity of $(La_{1-x}Sr_x)_yMnO_{3\pm\delta}$, Solid State Ionics 129 (2000) 145–162.

[20] J. Wu, X. Liu, Recent development of SOFC metallic interconnect, Journal of Materials Science and Technology 26 (2010) 293–305.